MIXED-PHASE SIMULATION WITH FRACTURE-PATH PREDICTION MODE FOR DYNAMICALLY CURVING FRACTURE

Toshihisa NISHIOKA, Takashi OKADA and Masahiro NAKATANI

Department of Ocean Mechanical Engineering
Kobe University of Mercantile Marine
5-1-1 Fukae Minamimachi, Higashinada-Ku, Kobe, 658, Japan

ABSTRACT

For non-self-similar fracture simulation, one of the present author previously proposed the concept of mixed-phase simulation. In this paper, the mixed-phase simulation with the fracture-path prediction mode is carried out for dynamically curving crack propagation occurred in a fracture test. The dynamic J integral is used for the evaluation of various mixed-mode fracture parameters for dynamically curving cracks. Simulated fracture paths are compared with the experimentally obtained actual one. Three propagation-direction criteria are postulated in the mixed-phase simulation. Among the postulated criteria, the local symmetry ($K_{II}=0$) criterion best predicts the actual fractured path.

KEYWORDS

Dynamic Fracture Mechanics, Moving Finite Element Method, Fast Fracture Mechanics, Dynamic J Integral, Component Separation Method, Mapping Technique, Dynamic Crack Propagation, Dynamic Crack Curving, Mixed-Phase Simulation, Fracture-Path Prediction Mode

INTRODUCTION

Dynamic fracture mechanics has mainly treated self-similar dynamic crack propagation. However, we often observe non-self-similar dynamic crack propagation such as dynamic crack curving and dynamic crack branching. So far, non-self-similar dynamic fracture mechanics has not been well established. Especially the simulation methodology for such non-self-similar crack propagation involves many inherent difficulties.

To accurately simulate fast curving fracture, Nishioka, Takemoto and Murakami (1989) developed a moving finite element method together with the concept of element-controlling plane. Using the moving finite element method, Nishioka, Murakami and Takemoto (1990) carried out the generation-phase simulation of fast curving fracture tests (Nishioka et al, 1990).

To characterize the fast curving fracture, we need two criteria, viz., a crack-propagation criterion and a propagation-direction criterion. Therefore, the application phase simulation should be conducted using postulated or predetermined these two criteria. However, crack-propagation criteria have several critical unsolved problems such as specimen-geometry dependence and crack-acceleration effects (Takahashi and Arakawa, 1987).

To verify each criterion separately, Nishioka (1996b) has proposed the concept of "*mixed phase simulation*" together with "*fracture-path prediction mode*" and "*crack-growth prediction mode*". In the fracture-path prediction mode, the crack is forced to extend according to the experimentally

recorded history of crack length or crack velocity, and a postulated propagation-direction criterion predicts the fracture path.

This paper presents important simulation techniques of the moving finite element method for the mixed-phase/fracture-path prediction mode simulation. The fracture path in the fast curving fracture test is predicted using several well-known propagation-direction criteria.

TYPES OF NUMERICAL SIMULATION FOR NON-SELF-SIMILAR FRACTURE PHENOMENA

For non-self-similar fracture such as curving crack growth, three types of numerical simulation can be considered, as proposed by Nishioka (1996b). First, the generation phase simulation can be conducted similarly with the generation phase simulation (Kanninen, 1978) for self-similar dynamic fracture, except additionally using experimental data on the curved fracture-path history (see Fig.1(a)).

On the other hand, in the application phase simulation for curving crack growth, two criteria must be postulated or predetermined as shown in Fig.1(b). One of them is the crack-propagation criterion that is almost same with the one used in the application phase simulation (Kanninen, 1978) for self-similar fracture. However, the crack-propagation criterion for the curving crack growth may involve mixed-mode fracture parameters. Thus, it should be described by a fracture parameter taking into account mixed-mode conditions, such as the dynamic J integral (Nishioka and Atluri, 1983). The other one is a criterion for predicting the direction of crack propagation (propagation-direction criterion or growth-direction criterion).

However, the application phase simulations of curving crack growth have not been fully, due to several critical difficulties in those simulations. For instance, in dynamic brittle fracture, the crack-propagation criterion described by fracture-toughness versus crack-velocity relation itself has the unsolved problems. Furthermore, the crack-propagation criteria may also be influenced by the geometry of fracture specimen.

To verify only the propagation-direction criterion such as the maximum energy release rate criterion, Nishioka (1996b) proposed "*mixed phase simulation*" as depicted in Fig.1. Regarding the crack-propagation history, the same experimental data for the a versus t relation used in the generation phase simulation can be used in the mixed-phase simulation. Thus, the increment of crack propagation is prescribed for the given time-step sizes in the numerical simulation. Then the propagation-direction criterion predicts the direction of fracture path in each time step. Simulated final fracture path will be compared with the experimentally obtained actual one. This mode of the mixed-phase simulation may be called "*fracture-path prediction mode*"(see Fig.1(c)-(i)).

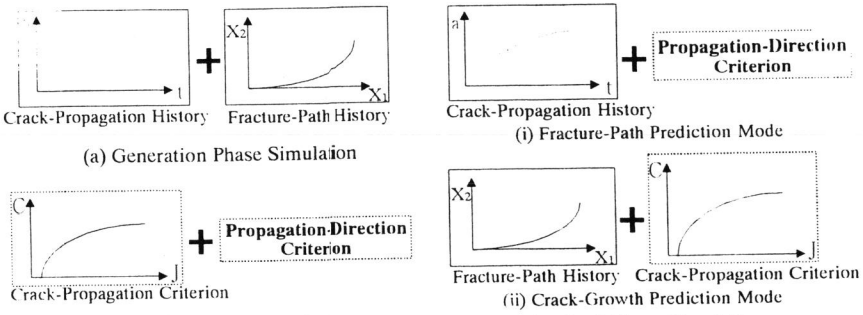

Fig.1 Mixed-phase simulation for non-self-similar dynamic fracture

Another mode of the mixed-phase simulation can be considered as depicted in Fig.1(c)-(ii), i.e., "*crack-growth prediction mode*". In this mode, the experimental data for the fracture-path history and the crack-propagation criterion are used simultaneously. In this case, the crack is forced to propagate along the actual fracture path during the numerical simulation. Simulated crack-propagation history should agree with the experimentally obtained actual one if the postulated crack-propagation criterion is valid.

MOVING FINITE ELEMENT METHOD FOR DYNAMICALLY CURVING CRACK PROPAGATION

To simulate dynamic crack curving, the curved crack path(s) should be modeled accurately by the finite element mesh pattern. Moreover, it is difficult to move a group of isoparametric elements around the crack-tip, in accordance with the curved fracture path. To overcome these difficulties, Nishioka, Takemoto and Murakami (1989) developed an automatic element-control method using a mapping technique. The concept of element-controlling plane is illustrated in Fig.2.

The procedures of the mesh movement and readjustment are controlled in the element-controlling plane. The mesh pattern in the real plane is created by the mapping from the element-controlling plane through a mapping function. The mapping function for the entire region consists of several Lagrangian elements. The shape functions of Lagrangian element (see Fig.3) can be constructed by

$$N_{kj}=L_k^m(\zeta)\cdot L_j^n(\lambda);\ (k=1, 2,\cdots, m;\ \text{and}\ j=1, 2,\cdots, n) \tag{1}$$

where $L_k^m(\zeta)$ and $L_j^n(\lambda)$ are Lagrange's polynomials, and can be written as

$$L_k^m(\zeta)=\frac{(\zeta-\zeta_1)\cdots(\zeta-\zeta_{k-1})(\zeta-\zeta_{k+1})\cdots(\zeta-\zeta_m)}{(\zeta_k-\zeta_1)\cdots(\zeta_k-\zeta_{k-1})(\zeta_k-\zeta_{k+1})\cdots(\zeta_k-\zeta_m)} \tag{2.a}$$

$$L_j^n(\lambda)=\frac{(\lambda-\lambda_1)\cdots(\lambda-\lambda_{j-1})(\lambda-\lambda_{j+1})\cdots(\lambda-\lambda_n)}{(\lambda_j-\lambda_1)\cdots(\lambda_j-\lambda_{j-1})(\lambda_j-\lambda_{j+1})\cdots(\lambda_j-\lambda_n)} \tag{2.b}$$

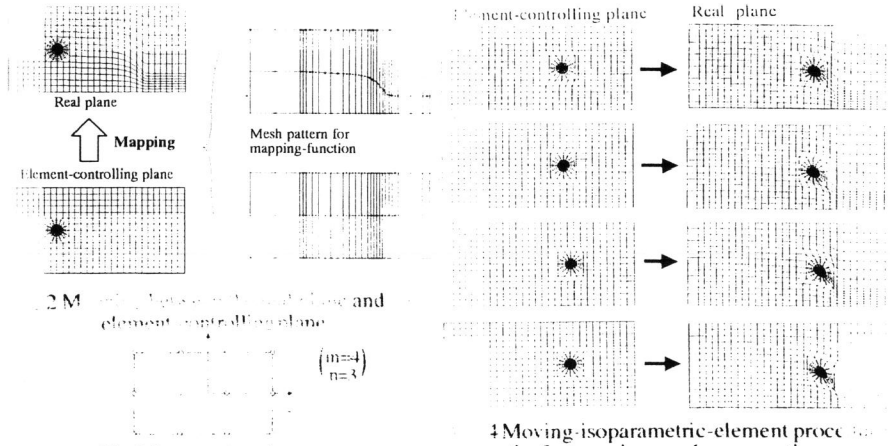

Fig.3 Lagrangian element

Fig.4 Moving-isoparametric-element procedure for fast curving crack propagation

in which ζ_k denotes the coordinate value of the k-th node in the ζ direction.

Any point $P_V(x_v, y_v)$ on the virtual element-controlling plane is mapped onto a point $P_r(x_r, y_r)$ on the real plane according to the following relation:

$$\begin{Bmatrix} x_r \\ y_r \end{Bmatrix} = \sum_{k=1}^{m} \sum_{j=1}^{n} N_{kj}(\zeta_v, \lambda_v) \begin{Bmatrix} x_{rkj} \\ y_{rkj} \end{Bmatrix} \tag{3}$$

where ζ_v, λ_v are the natural coordinates of the point $P_V(x_v, y_v)$ in the Lagrangian element, and (x_{rkj}, y_{rkj}) are the nodal coordinates of the Lagrangian element. As shown in Fig.2, the Lagrangian-element mapping function can be obtained by using only the coordinates of the crack path and the external boundaries.

In the moving element procedure, the mesh pattern for the elements near the crack-tip translates along the curved crack path in each time step for which crack growth occurs as illustrated in Fig.4. Thus, the crack-tip always remains almost at the center of the moving elements throughout the simulation. The regular isoparametric elements surrounding the moving elements are continuously distorted. To simulate a large amount of crack propagation, the mesh pattern around the moving elements is periodically readjusted, as is also shown in Fig.4.

THE DYNAMIC J INTEGRAL FOR DYNAMICALLY CURVING CRACKS

For dynamic cracks, Nishioka and Atluri (1983) derived the dynamic J integral (J') which has the following salient features:

(i) It physically represents the dynamic energy release rate;

(ii) It has the property of the path-independent integral, which gives a unique value for an arbitrary integral path surrounding the crack tip;

(iii) It can be related to the stress intensity factors by arbitrarily shrinking the integral path to the crack tip.

For a crack propagating at an angle θ_0 measured from the global X_1 axis (see Fig.5), the global components of dynamic J integral J'_k were derived by Nishioka and Atluri (1983) in a path-independent form:

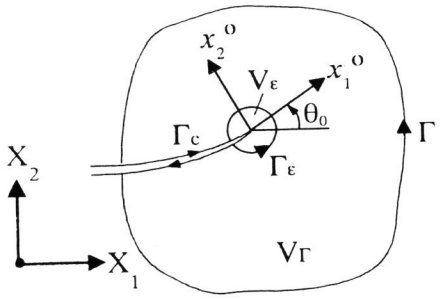

Fig.5 Integral paths and coordinate systems for a dynamically propagating crack

$$\begin{aligned} J'_k &= \lim_{\varepsilon \to 0} \int_{\Gamma_\varepsilon} [(W+K)n_k - t_i u_{i,k}]dS \\ &= \lim_{\varepsilon \to 0} \left\{ \int_{\Gamma+\Gamma_c} [(W+K)n_k - t_i u_{i,k}]dS + \int_{V_\Gamma - V_\varepsilon} [\rho \ddot{u}_i u_{i,k} - \rho \dot{u}_i \dot{u}_{i,k}]dV \right\} \end{aligned} \tag{4}$$

where W and K are the strain and kinetic energy densities, respectively, and $(\ )_{,k} \equiv \partial(\ )/\partial X_k$. Physically, the near-tip region V_ε can be considered as the process zone in which micro-processes associated with fracture occur.

Recent theoretical studies (Nishioka, 1989, Van Vroonheven, 1992, and Nishioka, 1994) lead to the following conclusions on the dynamic J integral.

(1) The dynamic J integral component $J_1^{'0}$ is "theoretically" invariant with respect to the shape of an infinitesimal process zone.

(2) The dynamic J integral component $J_2^{'0}$ is "practically" invariant with respect to the shape of an infinitesimal process zone.

(3) The other path-independent integrals that do not physically represent the dynamic energy release rate, are not invariant with respect to the shape of an infinitesimal process zone.

The above features of the dynamic J integral including its finiteness are very important for the theory and the numerical analyses in dynamic fracture mechanics.

In most numerical analyses, far-field integrals are usually used to evaluate the values of the dynamic J integral. In this case it is convenient to consider the following expression taking the limit of $V_\varepsilon \to 0$ ($\Gamma_\varepsilon \to 0$):

$$J'_k = \int_{\Gamma+\Gamma_c} [(W+K)n_k - t_i u_{i,k}]dS + \int_{V_\Gamma} [\rho \ddot{u}_i u_{i,k} - \rho \dot{u}_i \dot{u}_{i,k}]dV. \tag{6}$$

The crack-axis components of the dynamic J integral can be expressed by the following coordinate transformation:

$$J_l^{'0} = \alpha_{lk}(\theta_0)\, J'_k. \tag{5}$$

When the kinetic energy and the inertia forces in a cracked solid vanish, the dynamic J integral reduces to the static J integral (Rice, 1968, Budiansky and Rice, 1973). Thus, the dynamic J integral includes the static J integral as a special case.

The dynamic J integral can be related to the instantaneous stress intensity factors for the elastodynamically propagating crack with velocity C, as in (Nishioka and Atluri, 1983):

$$J_1^{'0} = \frac{1}{2\mu}\{A_I(C)K_I^2 + A_{II}(C)K_{II}^2 + A_{III}(C)K_{III}^2\} \tag{7}$$

$$J_2^{'0} = -\frac{A_{IV}(C)}{\mu} K_I K_{II} \tag{8}$$

where $(A_I, \ldots, A_{IV})$ are functions of the crack velocity.

Various procedures for determining mixed-mode dynamic stress-intensity factors from the dynamic J integral values were summarized in (Nishioka, 1996a). The typical procedures are (i) direct method, (ii) mode decomposition method, (iii) component separation method.

To overcome the difficulties in the direct method and in the mode decomposition method, the component separation method was proposed by Nishioka, Murakami and Takemoto (1990). If non-singular regular elements are used around the crack tip under a mixed-mode condition, the value of $J_2^{'0}$ cannot be obtained accurately owing to the finiteness of the energy densities in the regular elements. However, the $J_1^{'0}$ component is not affected by the modeling of the crack tip, and can be evaluated accurately (Nishioka, Murakami and Takemoto, 1990), even by the global components of the dynamic J integral, J'_k (k=1, 2). The formulae of the component separation method can be expressed by

$$K_I = \delta_I \left\{ 2\mu J_1^{'0} \beta_2 \Big/ \left[A_I \left(\delta_I^2 \beta_2 + \delta_{II}^2 \beta_1 \right) \right] \right\}^{1/2} = \delta_I \left\{ 2\mu\beta_2 \left(J'_1 \cos\theta_0 + J'_2 \sin\theta_0 \right) \Big/ \left[A_I \left(\delta_I^2 \beta_2 + \delta_{II}^2 \beta_1 \right) \right] \right\}^{1/2} \tag{9}$$

$$K_{II}=\delta_{II}\left\{2\mu J'^{0}_{1}\beta_1\Big/\left[A_{II}\left(\delta_I^2\beta_2+\delta_{II}^2\beta_1\right)\right]\right\}^{1/2}=\delta_{II}\left\{2\mu\beta_1\left(J'_1\cos\theta_0+J'_2\sin\theta_0\right)\Big/\left[A_{II}\left(\delta_I^2\beta_2+\delta_{II}^2\beta_1\right)\right]\right\}^{1/2} \quad (10)$$

in which δ_I and δ_{II} are the mode I and mode II crack-opening displacements near the crack tip.

MIXED-PHASE SIMULATION WITH FRACTURE-PATH PREDICTION MODE

Figure 6 shows a typical fractured specimen obtained in fast curving fracture experiments (Nishioka et al, 1990). Figure 7 shows the history of fast curving crack propagation that was measured by a high-speed camera in the experiment. In the figure, a_x and a_y denote the global coordinates of the instantaneous crack-tip position. The maximum crack velocity was approximately 300 m/sec. The crack attested at t=1264 μsec.

The results of the generation-phase simulations of fast curving fracture experiments have been already reported by Nishioka et al (1991) and Nishioka (1995). For the sake of comparison, the K_I and K_{II} values obtained by the generation phase simulation are shown in Fig.8.

Next, the mixed-phase simulation with the fracture-path prediction mode for the fast curving fracture experiment is explained. Figure 9 schematically explains the numerical procedures for the path-prediction mode of the mixed-phase simulation. In each time step, the crack is advanced by the small increment according with the experimental history (crack-length versus time curve). The fracture path is predicted as follows: At a generic time step n, as the first trial, the crack is advanced in the tangential direction at the crack tip of the step n-1. If an employed propagation-direction criterion, for example the maximum K_I criterion, is satisfied at the attempted crack tip

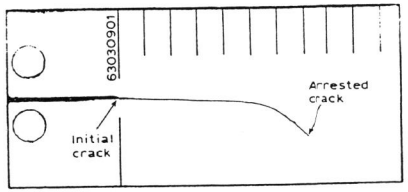

Fig.6 Dynamically curved fracture specimen

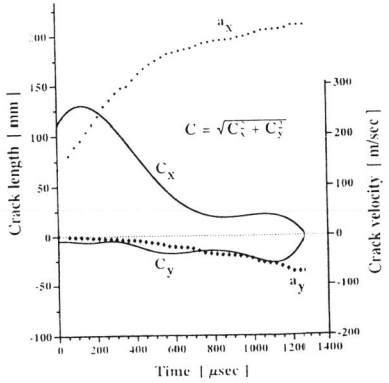

Fig.7 Experimental data of fast curving fracture

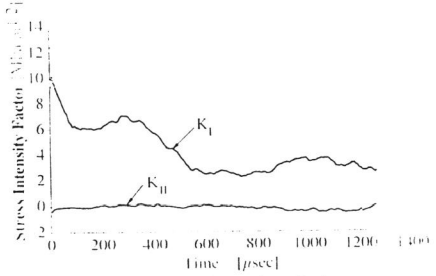

(generation phase simulation)

Fig.8 Variations of stress intensity factors during fast curving fracture

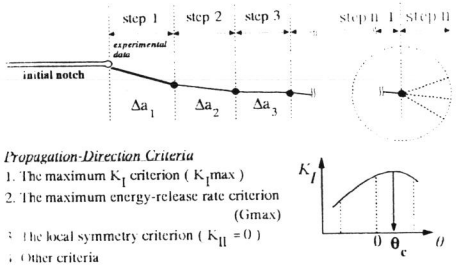

Fig.9 Procedures for fracture-path prediction

location, the crack is advanced in this direction. If not, K_I values are evaluated at the other two crack tips in attempted directions as shown in Fig.9. Then the fracture direction θ_c that exactly satisfies the employed propagation-direction criterion is determined by the K_I versus θ curve.

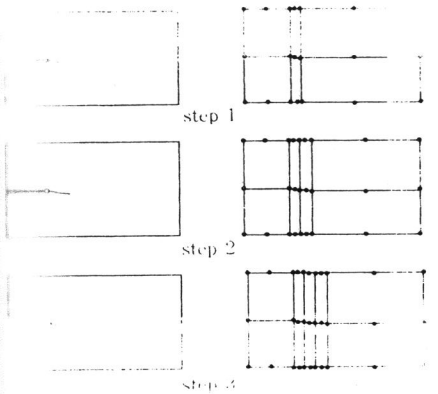

Fig.10 Automatic mesh control

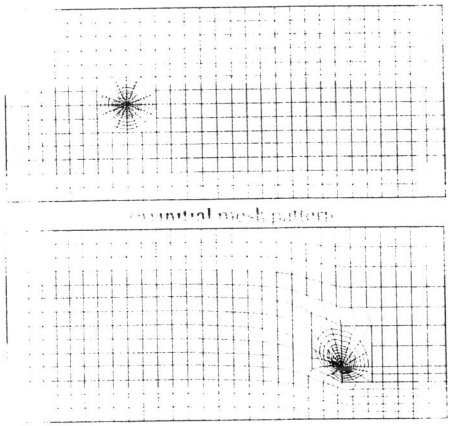

(b) final mesh pattern

Fig.11 Moving finite element mesh patterns

To accommodate the dynamically curving crack and the moving finite elements, the mesh pattern for Lagrange mapping function is continuously varied, as schematically illustrated in Fig.10. Figures 11(a) and (b) show the initial mesh pattern (t=0) and the final mesh pattern at the time of crack arrest, respectively. During the simulation, the web-like mesh moves in a similar manner explained in Fig.4.

The global components of the dynamic J integral J'_1 and J'_2 were evaluated along the circular paths in the web-like mesh (see Fig.11). Excellent path independence of the dynamic J integral values were obtained throughout the simulations. Then these dynamic J integral values were converted to the dynamic stress intensity factors by using the component separation method (see eqns (9) and (10)).

All simulated fracture paths are compared with the experimental one in Fig.12. As long as the criteria tested here, the local symmetry criterion ($K_{II}=0$ criterion) predicts the closest fracture path to the experimental one.

The numerical results of the K_I and K_{II} values obtained by the mixed-phase simulations are shown in Figs.13(a)-(c). As seen from the figures, in each case, K_I decreases rapidly after the

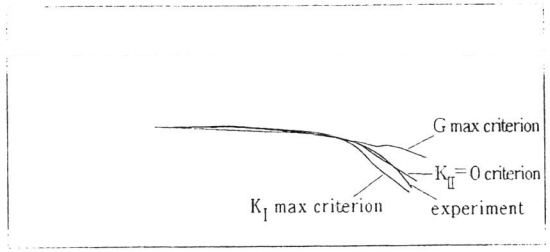

Fig.12 Simulated fracture paths

crack extension. After certain crack extension, the crack propagates with a nearly constant K_I value. In all cases, the values of K_{II} are relatively small compared with those of K_I even in the cases of the Gmax and $K_I$max criteria although those criteria predict somewhat deviated fracture paths as indicated in Fig.12.

CONCLUDING REMARKS

The concept of the mixed-phase/fracture-path prediction mode simulation was presented together with the simulation results for the fast curving fracture test. Among the propagation-direction criteria implemented in the mixed-phase simulation, the local symmetry criterion best predicted the actual fractured path.

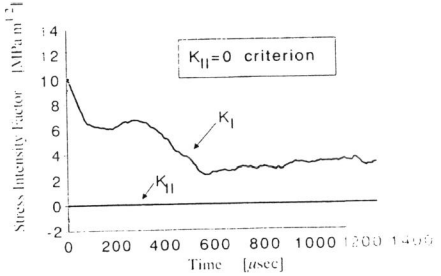

(a) the local symmetry criteri

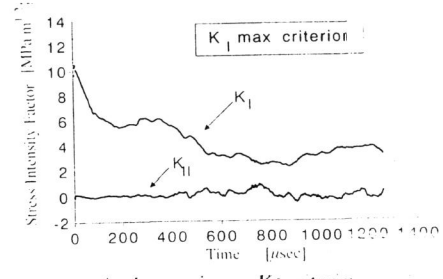

(b) the maximum K_I criterion

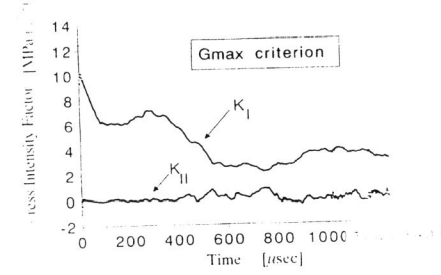

the maximum energy-release rate criterion

(mixed-phase/path-prediction modesimulation)
Fig.13 Variations of stress intensity factors during fast curving

REFERENCES

Budiansky, B. and Rice, J.R., 1973, Journal of Applied Mechanics, **40**, 201-203.

Kanninen, M.F., 1978, *Numerical Methods in Fracture Mechanics*, (D.R.J. Owen and A.R. Luxmoore, eds.), Pineridge Press, 612-634.

Nishioka, T. and Atluri, S.N., 1983, *Eng. Fract. Mech.*, **18**, 1-22.

Nishioka, T., 1989, *Eng. Fract. Mech.*, **32**, 309-319.

Nishioka, T., Takemoto, Y. and Murakami, R., 1989, Dynamic Fracture Mechanics For the 1990's, ASME Publication PVP-Vol.160, 117-125.

Nishioka, T., Kittaka, H., Murakami, T. and Sakakura, K., 1990, *Int. J. Pres. Ves. & Piping*, **44**, 17-33.

Nishioka, T., Murakami, R. and Takemoto, Y., 1990, *Int. J. Pres. Ves. & Piping*, **44**, 329-352.

Nishioka, T., Murakami, R., Murakami, T., and Sakakura, K., 1991, *Dynamic Failure of Materials -Theory, Experiments and Numerics-*, (H.P. Rossmanith and A.J. Rosakis, eds.), Elsevier Applied Science, 232-247.

Nishioka, T., 1994, *JSME Int. J.*, Series A, **37**, 313-333.

Nishioka, T., 1995, *Recent Developments in Dynamic Fracture Mechanics*, (M.H. Aliabadi, ed.), Computational Mechanics Publications, Chapter 1, 1-60.

Nishioka, T., 1996a, *Fracture: A Topical Encyclopedia of Current Knowledge Dedicated to Alan Arnold Griffith*, (G.P. Cherepanov, ed.), Krieger Publishing Company, 536-572.

Nishioka, T., 1996b, *Optics and Laser Engineering*, Special Issue on Hybrid Methods in Experimental Mechanics (to appear).

Rice, J.R., 1968, *Journal of Applied Mechanics*, 35, 379-386.

Takahashi, K. and Arakawa, K., 1987, *Experimental Mechanics*, **27**, 195-200.

Van Vroonheven, J.C.W., 1992, *Reliability and Structural Integrity of Advanced Materials*, Bulgaria, 885-890.